Inorg. Chem. **2004**, *43*, 2132–2140

Oxamidate-Bridged Dinuclear Five-Coordinate Nickel(II) Complexes: A Magneto–Structural Study

M. Dolores Santana,[†] Gabriel García,*[,†] Miguel Julve,*[,‡] Francesc Lloret,[‡] José Pérez,[§] Malva Liu,[||] Francisco Sanz,[||] Joan Cano,[⊥] and Gregorio López[†]

Departamento de Química Inorgánica, Universidad de Murcia, 30071 Murcia, Spain, Departament de Química Inorgánica/Instituto de Ciencia Molecular, Facultad de Química, Universitat de València, Avda. Dr. Moliner 50, 46100 Burjassot (València), Spain, Departamento de Ingeniería Minera, Geológica y Cartográfica, Universidad Politécnica de Cartagena, 30203 Cartagena, Spain, Departament de Termodinámica, Universitat de València, 46100 Burjassot (València), Spain, and Laboratoire de Chimie Inorganique, UMR 8613, CNRS, Université de Paris-Sud, 91405 Orsay, France

Received February 5, 2003

The preparation, spectroscopic characterization, and magnetic study of three new oxamidate-bridged nickel(II) dinuclear complexes of formulas $\{[Ni(Me_3[12]aneN_3)]_2(\mu\text{-oa})\}(PF_6)_2$ (**1**), $\{[Ni(Me_3[12]aneN_3)]_2(\mu\text{-dmoa})\}(PF_6)_2$ (**2**), and $\{[Ni(Me_3[12]aneN_3)]_2(\mu\text{-dpoa})\}(PF_6)_2$ (**3**) ($Me_3[12]aneN_3$ = 2,4,4-trimethyl-1,5,9-triazacyclododec-1-ene, oa = oxamidate, dmoa = *N*,*N*′-dimethyloxamidate, and dpoa = *N*,*N*′-diphenyloxamidate) are reported. The crystal structures of two of them (**1** and **3**) have been determined. **1** and **3** crystallize in the monoclinic system, space group $P2_1/c$, with $Z = 2$ and $a = 7.901(4)$ Å, $b = 13.597(6)$ Å, $c = 17.565(10)$ Å, and $\beta = 96.46(4)°$ for **1** and $a = 13.854(3)$ Å, $b = 17.469(4)$ Å, $c = 12.543(3)$ Å, and $\beta = 116.22(3)°$ for **3**. The structures of **1** and **3** consist of dinuclear $\{[Ni(Me_3[12]aneN_3)]_2(\mu\text{-oa})\}^{2+}$ and $\{[Ni(Me_3[12]aneN_3)]_2(\mu\text{-dpoa})\}^{2+}$ cations and hexafluorophosphate anions. Each nickel in **1**–**3** is five-coordinate, and the substitution of the hydrogen atom of the amidate nitrogen of **1** by a methyl (**2**) or a phenyl (**3**) group causes a significant modification of the stereochemistry of the nickel(II) ions from square pyramidal toward trigonal bipyramidal (τ values of 0.12 and 0.48 for **1** and **3**, respectively). The NOESY spectrum of **3** has allowed us to achieve the assignment of the phenyl protons of the *N*,*N*′-diphenyloxamidate. The value of magnetic coupling between the two nickel(II) ions across the oxamidate bridge [$J = -57.0$ (oa, **1**), -38.0 (dmoa, **2**) and -30.5 cm^{-1} (dpoa, **3**)] is very sensitive to this stereochemical change, and its variation is explained on the basis of orbital considerations. DFT type calculations have been performed to analyze and substantiate the trend of the magnetic coupling in **1**–**3**.

Introduction

Studies of magnetic spin exchange in di- and polynuclear metal complexes in terms of stereochemical factors and nature of bridging groups are of current interest.[1] It is known that the oxamide dianion can adopt bidentate and bis-bidentate coordination modes in its metal complexes to yield either mono-[2] or polynuclear[3] compounds. In particular, some oxamidate-bridged dinuclear copper(II) complexes are known[3b,c,e,g,4,5] and it is established that the oxamidate bridge can mediate a stronger antiferromagnetic coupling than the oxalate bridge.[3b,e−g] Square-planar diamagnetic species are

[†] Departamento de Química Inorgánica, Universidad de Murcia, 30071 Murcia, Spain. E-mail: ggarcia@um.es.
[‡] Departament de Química Inorgánica/Instituto de Ciencia Molecular, Facultad de Química, Universitat de Valéncia, Avda. Dr. Moliner 50, 46100 Burjassot (Valéncia), Spain. E-mail: miguel.julve@uv.es.
[§] Departamento de Ingeniería Minera, Geológica y Cartográfica, Universidad Politécnica de Cartagena, 30203 Cartagena, Spain.
[||] Departament de Termodinámica, Universitat de Valéncia, 46100 Burjassot (Valéncia), Spain.
[⊥] Laboratoire de Chimie Inorganique, UMR 8613, CNRS, Université de Paris-Sud, 91405 Orsay, France.

(1) See, for example: (a) Kahn, O. *Molecular Magnetism*; VCH: New York, 1993. (b) O'Connor, C. J. *Prog. Inorg. Chem.* **1982**, *29*, 303. (c) Melnic, M. *Coord. Chem. Rev.* **1982**, *42*, 259. (d) Kahn, O. *Adv. Inorg. Chem.* **1995**, *43*, 179.
(2) (a) Hoffmann, K. A.; Ehrardt, U. *Ber. Dtsch. Chem. Ges.* **1913**, *46*, 1457. (b) Rising, M.; Hicks, J. S.; Moarke, G. A. *J. Biol. Chem.* **1930**, *89*, 1. (c) Poddubnaya, N. S.; Gabrilov, N. L.; Obshck, Z. *Khim.* **1948**, *18*, 1848. (d) Kuroda, Y.; Kato, M.; Sone, K. *Bull. Chem. Soc. Jpn.* **1961**, *34*, 877. (e) Armendarez, P. X.; Nakamoto, K. *Inorg. Chem.* **1966**, *5*, 796.

10.1021/ic030050f CCC: $27.50
Published on Web 02/26/2004

obtained in the case of oxamidate-contained nickel(II) complexes due to the coordination of strong-field amide N atoms. This fact explains the lack of magnetic studies concerning these complexes[6a] in contrast to the relevant magneto−chemical role played by the corresponding copper(II) compounds.[6,7] However, the diamagnetic mononuclear nickel(II) units have been used as bidentate ligands to prepare dinuclear oxamidate-bridged nickel(II) complexes in which the two nickel(II) atoms have different environments, one located in a square planar environment, while the other was in an octahedral geometry.[8,9] Moreover, paramagnetic nickel(II) oxamide complexes have been achieved when the strength of the ligand field of the substituted oxamide was decreased by choosing the nature of the donor group (carboxylate instead of amine nitrogen or pyridine for instance).[6] In an attempt to obtain oxamidate-bridged low-dimensional nickel(II) complexes, trinuclear species have been reported in which the two external nickel units are diamagnetic and the central one has nickel(II) octahedrally coordinated.[10] Studies dealing with the formation and the structural investigation of binuclear metal complexes bridged by the oxamidate group containing pentacoordinate nickel(II) are limited to nickel(II)−copper(II) heterodinuclear complexes,[11] but no similar study has been found for pentacoordinate nickel(II) ions in homodinuclear complexes. In this paper we report the preparation, structure, and spectroscopic and magnetic behavior of dinuclear oxamidate-bridged nickel(II) complexes, in which the two nickel(II) atoms are in a pentacoordinate environment.

Experimental Section

All chemicals were of reagent grade and were used without further purification. Solvents were dried and distilled by general methods before use.

Ligands and Complexes Preparations. The ligands *N*,*N*′-bis(substituent)oxamides were synthesized by the following experimental procedure:[12] Oxalyl dichloride (10 mmol) in anhydrous tetrahydrofuran (25 mL) was added dropwise to an anhydrous tetrahydrofuran solution (50 mL) of the appropriate amine (20 mmol) and triethylamine (2 mmol) cooled in an ice bath. The resulting suspension was stirred at room temperature for 24 h. The white precipitate was filtered off; the tetrahydrofuran solution was partially evaporated under reduced pressure, and a white precipitate was obtained. It was filtered off, washed with diethyl ether, and dried in vacuo. The melting points of the ligands are 216 °C (MeHNCOCONHMe, H_2dmoa) and 255 °C (PhHNCOCONHPh, H_2dpoa). The complex $[Ni(Me_3[12]aneN_3)(\mu\text{-}OH)]_2(PF_6)_2$ ($Me_3[12]aneN_3$ = 2,4,4-trimethyl-1,5,9-triazacyclododec-1-ene) was prepared by the previously described procedure.[13]

{[Ni(Me$_3$[12]aneN$_3$)]$_2$(μ-oa)}(PF$_6$)$_2$ (1). To a suspension of $[Ni(Me_3[12]aneN_3)(\mu\text{-}OH)]_2(PF_6)_2$ (0.150 g, 0.170 mmol) in acetone (20 mL) was added $H_2NCOCONH_2$ (0.015 g, 0.170 mmol). The mixture was stirred at room temperature for 30 min and under reflux for 2 h. Acetone was evaporated under reduced pressure until ca. 10 mL, and the addition of diethyl ether (15 mL) resulted in the formation of a light blue-violet solid which was filtered off, washed with diethyl ether, and air-dried. Yield: 0.129 g (81%). Anal. Calcd for $C_{26}H_{52}N_8O_2P_2F_{12}Ni_2$: C, 34.1; H, 5.7; N, 12.2. Found: C, 34.4; H, 5.6; N, 12.2. FAB (+ve): *m*/*z* 769 $[M]^+$, 623 $[M]^{2+}$. λ_{max} [nm (ϵ); acetone]: 582 (109), 361 (397). IR (cm^{-1}, Nujol): 3350 ($\nu_{N-Hoxamidate}$), 3290 (ν_{N-Hmc}), 1660 ($\nu_{C=Nmc}$), 1608 ($\nu_{C-Ooxamidate}$). ^{1}H NMR (acetone-d_6) [δ (ppm)]: 289.7 (H_α), 188.8 (H_α), 143.1 (H_α), 141.5 (H_α), 71.3 (H_α), 38.4 (4-Me, 3H), 27.2 (H_α), 23.9 (H_α), 20.6 (H_α), 18.4 (4-Me, 3H), −8.4 (H_β, 2H), −9.4 (H_β), −10.1 (2-Me, 3H), −22.4 (H_β), −22.6 (H_β), −23.6 (H_β).

{[Ni(Me$_3$[12]aneN$_3$)]$_2$(μ-dmoa)}(PF$_6$)$_2$ (2). The compound H_2dmoa (0.020 g, 0.176 mmol) was added to a suspension of $[Ni(Me_3[12]aneN_3)(\mu\text{-}OH)]_2(PF_6)_2$ (0.152 g, 0.176 mmol) in acetone (30 mL). The mixture was stirred under reflux for 1 h and at room temperature for 24 h. Acetone was removed under reduced pressure until ca. 15 mL, and the addition of diethyl ether (8 mL) resulted in the formation of a light blue solid, which was filtered off, washed with diethyl ether, and air-dried. Yield: 0.119 g (72%). Anal. Calcd for $C_{28}H_{56}N_8O_2P_2F_{12}Ni_2$: C, 35.6; H, 6.0; N, 11.9. Found: C, 35.2; H, 5.9; N, 11.3. FAB (+ve): *m*/*z* 652 $[M]^{2+}$. λ_{max} [nm (ϵ); acetone]: 597 (104), 378 (528). IR (cm^{-1}, Nujol): 3292, 3250 (ν_{N-Hmc}), 1662 ($\nu_{C=Nmc}$), 1614 ($\nu_{C-Ooxamidate}$). ^{1}H NMR (acetone-d_6) [δ (ppm)]: 302.9 (H_α), 189.2 (H_α), 162.9 (H_α), 136.4 (H_α), 89.3 ($Me_{oxamidate}$, 3H), 79.9 (H_α), 75.1 (H_α), 38.6 (4-Me, 3H), 25.7 (H_α), 25.2 (H_α), 17.8 (4-Me, 3H), −7.8 (H_β), −9.0 (H_β), −9.3 (H_β), −11.0 (2-Me, 3H), −25.1 (H_β, 2H), −25.9 (H_β).

(3) (a) Nonoyama, K. Doctoral Thesis, Gakushūin University, Tokyo, 1985; No. 43. (b) Nonoyama, K.; Ojima, H.; Ohki, K.; Nonoyama, M. *Inorg. Chim. Acta* **1980**, *41*, 155. (c) Sletten, J. *Acta Chem. Scand.* **1982**, *A36*, 345. (d) Sletten, J. *Acta Chem. Scand.* **1985**, *A39*, 475. (e) Bencini, A.; Benelli, C.; Gatteschi, D.; Zanchini, C.; Fabretti, A. C.; Franchini, G. C. *Inorg. Chim. Acta* **1984**, *86*, 169. (f) Verdaguer, M.; Kahn, O.; Julve, M.; Gleizes, A. *Nouv. J. Chim.* **1985**, *9*, 325. (g) Ojima, H.; Nonoyama, K. *Coord. Chem. Rev.* **1988**, *92*, 85. (h) Soto, L.; García, J.; Escrivá, E.; Legros, J.-P.; Tuchagues, J.-P.; Dahan, F.; Fuertes, A. *Inorg. Chem.* **1989**, *28*, 3378. (i) Okawa, H.; Matsumoto, N.; Koikawa, M.; Takeda, K.; Kida, S. *J. Chem. Soc., Dalton Trans.* **1990**, 1383.

(4) Bencini, A.; Vaira, M. D.; Fabretti, A. C.; Gatteschi, D.; Zanchini, C. *Inorg. Chem.* **1984**, *23*, 1620.

(5) Journaux, Y.; Sletten, J.; Kahn, O. *Inorg. Chem.* **1986**, *25*, 439.

(6) (a) Lloret, F.; Sletten, J.; Ruiz, R.; Julve, M.; Faus, J.; Verdaguer, M. *Inorg. Chem.* **1992**, *31*, 778. (b) Ruiz, R.; Faus, J.; Lloret, F.; Julve, M.; Journaux, Y. *Coord. Chem. Rev.* **1999**, *193*−*195*, 1069.

(7) (a) Lloret, F.; Julve, M.; Real, J. A.; Faus, J.; Ruiz, R.; Mollar, M.; Castro, I.; Bois, C. *Inorg. Chem.* **1992**, *31*, 2956. (b) Real, J. A.; Ruiz, R.; Faus, J.; Lloret, F.; Julve, M.; Journaux, Y.; Philoche-Levisalles, M.; Bois, C. *J. Chem. Soc., Dalton Trans.* **1994**, 3769. (c) Chen, Z. N.; Qiu, J.; Wu, Z. K.; Fu, D. G.; Yu, K. B.; Tang, W. X. *J. Chem. Soc., Dalton Trans.* **1994**, 1923. (d) Lloret, F.; Julve, M.; Faus, J.; Ruiz, R.; Castro, I.; Mollar, M.; Philoche-Levisalles, M. *Inorg. Chem.* **1992**, *31*, 784. (e) Chen, Z. N.; Liu, S. X.; Qiu, J.; Wang, Z. M.; Huang, J. L.; Tang, W. X. *J. Chem. Soc., Dalton Trans.* **1994**, 2989. (f) Sanz, J. L.; Cervera, B.; Ruiz, R.; Bois, C.; Faus, J.; Lloret, F.; Julve, M. *J. Chem. Soc., Dalton Trans.* **1996**, 1359. (g) Bencini, A.; Benelli, C.; Fabretti, A. C.; Franchini, G. C.; Gatteschi, D. *Inorg. Chem.* **1986**, *25*, 1063. (h) Chen, Z. N.; Wang, J. L.; Qiu, J.; Miao, F. M.; Tang, W. X. *Inorg. Chem.* **1995**, *34*, 2255. (i) Chen, Z. N.; Fu, D. G.; Yu, K. B.; Tang, W. X. *J. Chem. Soc., Dalton Trans.* **1994**, 1917. (j) Chen, Z. N.; Qiu, J.; Tang, W. X.; Yu, K. B. *Inorg. Chim. Acta* **1994**, *224*, 171. (k) Dominguez-Vera, J. M.; Galvez, N.; Colacio, E.; Cuesta, R.; Costes, J. P.; Laurent, J. P. *J. Chem. Soc., Dalton Trans.* **1996**, 861.

(8) Chen, Z. N.; Tang, X. W.; Chen, J.; Zheng, P. J.; Chen, C. G.; Yu, K. B. *Polyhedron* **1994**, *13*, 873.

(9) Wei, P.-R.; Jia, L.; Liu, C.-R.; Han, Q.; Wei, G.-C.; Gao, S. *Polyhedron* **1995**, *14*, 441.

(10) (a) Fabretti, A. C.; Giusti, A.; Albano, V. G.; Castellari, C.; Gatteschi, D.; Sessoli, R. *J. Chem. Soc., Dalton Trans.* **1991**, 2133. (b) Chen, Z.-N.; Zhang, H.-X.; Yu, K.-B.; Su, C.-Y.; Kang, B.-S. *Polyhedron* **1998**, *17*, 1535.

(11) Escuer, A.; Vicente, R.; Ribas, J.; Costa, R.; Solans, X. *Inorg. Chem.* **1992**, *31*, 2627.

(12) Casellato, U.; Guerriero, P.; Tamburini, S.; Vigato, P. A. *Inorg. Chim. Acta* **1997**, *260*, 1.

(13) (a) Martin, J. W. L.; Johnston, J. H.; Curtis, N. F. *J. Chem. Soc., Dalton Trans.* **1978**, 68. (b) Escuer, A.; Vicente, R.; Ribas, J. *Polyhedron* **1992**, *11*, 453.

{[Ni(Me$_3$[12]aneN$_3$)]$_2$(μ-dpoa)}(PF$_6$)$_2$·2(CH$_3$)$_2$CO (3). To a suspension of [Ni(Me$_3$[12]aneN$_3$)(μ-OH)]$_2$(PF$_6$)$_2$ (0.159 g, 0.184 mmol) in acetone (25 mL) was added H$_2$dpoa (0.044 g, 0.184 mmol). The mixture was stirred under reflux for 45 min and at room temperature for 24 h. Acetone was removed under reduced pressure until ca. 10 mL, and the addition of diethyl ether (10 mL) resulted in the formation of a light blue solid, which was filtered off, washed with diethyl ether, and air-dried. Yield: 0.153 g (78%). Anal. Calcd for $C_{44}H_{72}N_8O_4P_2F_{12}Ni_2$: C, 44.6; H, 6.1; N, 9.5. Found: C, 44.5; H, 6.0; N, 9.7. FAB (+ve): *m*/*z* 921 $[M]^+$, 776 $[M]^{2+}$. λ_{max} [nm (ϵ); acetone]: 589 (131), 361 (689). IR (cm^{-1}, Nujol): 3290, 3252 (ν_{N-Hmc}), 1654 ($\nu_{C=Nmc}$), 1610 ($\nu_{C-Ooxamidate}$), 1586. ^{1}H NMR (acetone-d_6) [δ (ppm)]: 247.3 (H$_\alpha$), 159.1 (H$_\alpha$, 2H), 132.4 (d, H$_\alpha$), 108.5 (d, H$_\alpha$), 77.0 (H$_\alpha$, 2H), 50.5 (d, H$_\alpha$), 39.6 (4-Me, 3H), 25.6 (H$_o$, 2H), 17.5 (H$_\alpha$), 15.4 (4-Me, 3H), −3.1 (H$_m$, 2H), −3.4 (H$_p$), −9.1 (H$_\beta$), −9.7 (H$_\beta$), −11.3 (H$_\beta$), −11.9 (2-Me, 3H), −17.6 (H$_\beta$), −20.4 (H$_\beta$), −24.0 (H$_\beta$).

Physical Techniques. C, H, and N analyses were carried out with a Carlo Erba model EA 1108 microanalyzer. IR spectra were recorded on a Perkin-Elmer 16F PC FT-IR spectrophotometer using Nujol mulls between polyethylene sheets. The NMR spectra of (CD$_3$)$_2$CO solutions were recorded on a Bruker model AC 200E or a Bruker AV-400 spectrometer. NOESY spectra were recorded on the Bruker 400 MHz spectrometer at 21 °C in (CD$_3$)$_2$CO solutions using 256 individual FID's with 4096 scans each. The mixing time was varied in the 9−50 ms range. Experimental parameters were varied to obtain best resolution and the signal-to-noise. The UV/vis spectra (in acetone) were recorded on a Hitachi 2000V spectrophotometer for the 300−800 nm range. Fast atom bombardment (FAB) mass spectra were run on a Fisons VG Autospec spectrometer operating in the FAB$^+$ mode. The magnetic susceptibility of polycrystalline samples of **1**−**3** were measured in the temperature range 2−300 K with a Quantum Design SQUID magnetometer under an applied magnetic field of 1 T. The device was calibrated with (NH$_4$)$_2$Mn(SO$_4$)$_2$·6H$_2$O. Corrections for the diamagnetism of **1**−**3** were estimated from Pascal constants[14] as -461×10^{-6} (**1**), -485×10^{-6} (**2**), and -528×10^{-6} cm^3 mol^{-1} (**3**), respectively. Experimental susceptibilities were also corrected for the temperature-independent paramagnetism [-100×10^{-6} cm^3 mol^{-1}/Ni(II)].

Computational Details. A detailed description of the computational strategy adopted in this work has been described elsewhere[15] and is only briefly outlined here. For the evaluation of the coupling constant of dinuclear models, two separate calculations are carried out by means of density functional theory,[16] one for the triplet and another for the singlet state. The hybrid B3LYP method,[17] as implemented in Gaussian98,[18] has been used in all calculations, mixing the exact Hartree−Fock exchange[19] with Becke's expression for the exchange and with the Lee−Yang−Parr correlation functional.[20] Double-ζ quality and triple-ζ quality basis sets proposed by Ahlrichs[21] have been employed for nonmetallic and metallic atoms, respectively. Also, for the metallic atoms, we have added two extra polarization p functions. The presence of a low-energy excited singlet makes it difficult to evaluate accurately the energy of the lowest singlet by a single-determinant method. To solve this problem, broken-symmetry wave functions, as proposed by Noodleman et al., have been used.[22−24] Previously, it has been found that, among the most common functionals, the B3LYP method combined with the broken-symmetry treatment is the strategy which provides the best results for calculating coupling constants.[15,25−29] It is clear that for broken-symmetry Hartree−Fock calculations it is necessary to make a correction due to the multideterminant character of the wave function of the low-multiplicity state.[29] On the other hand, for DFT calculations we adopt single-determinant wave functions for which DFT is well defined.[30−33] Then, we use the broken-symmetry energy calculated by DFT methods as the real energy of the state.

Crystallographic Data Collection and Structure Determination. Crystals suitable of **1** and **3** for a diffraction study were prepared by slow diffusion of diethyl ether into their acetone solution. Data collection was performed on a Siemens Smart CCD diffractometer using graphite-monochromated Mo Kα radiation (λ = 0.710 73 Å) with a nominal crystal to detector distance of 4.0 cm. The crystal data are summarized in Table 1. Single crystals of dimensions 0.4 × 0.01 × 0.01 mm^3 for **1** and 0.4 × 0.1 × 0.1 mm^3 for **3** were mounted on a glass fiber in a random orientation. For compound **1** the data collection was performed at −100 °C and the diffraction data were collected on the basis of one ω-scan run (starting $\omega = -28°$) at $\phi = 0$ with the detector at $2\theta = 28°$. A total of 606 frames were collected at 0.3° intervals and 60 s/frame. The crystal decomposes after 10 h of exposure to X-rays. For complex **3** an hemisphere of data was collected on the basis of three ω-scans runs (starting $\omega = -28°$) at values $\phi = 0$, 90, and 180° with the detector at $2\theta = 28°$. At each of these runs, frames (606, 435, and 230 respectively) were collected at 0.3° intervals and 20 s/frame. The diffraction frames were integrated using the SAINT package[34] and corrected for absorption with SADABS.[35] The raw intensity data were converted (including corrections for Lorentz and polarization effects) to structure amplitudes and their esd's using the SAINT program. The structures were solved by direct methods[36] and refined[36] by full-matrix least-squares techniques using anisotropic thermal parameters for non-H atoms.

Results and Discussion

Synthesis of 1−3. The pentacoordinate oxamidate complexes of nickel(II) were obtained from reaction mixtures of [Ni([12]aneN$_3$)(μ-OH)]$_2$(PF$_6$)$_2$ and oxamide or *N*,*N*′-bis-

(14) Earnshaw, A. *Introduction to Magnetochemistry*; Academic Press: London and New York, 1968.
(15) Ruiz, E.; Alemany, P.; Alvarez, S.; Cano, J. *J. Am. Chem. Soc.* **1997**, *119*, 1297.
(16) Parr, R. G.; Yang, W. *Density-Functional Theory of Atoms and Molecules*; Oxford University Press: New York, 1989.
(17) Becke, A. D. J. *J. Chem. Phys.* **1993**, *98*, 5648.
(18) *Gaussian 98*, rev. A.11; Gaussian, Inc.: Pittsburgh, PA, 1998.
(19) Becke, A. D. J. *Phys. Rev.* **1988**, *A38*, 3098.
(20) Lee, C.; Yang, W.; Parr, R. G. *Phys. Rev.* **1988**, *B37*, 785.
(21) Schaefer, A.; Horn, H.; Ahlrichs, R. *J. Chem. Phys.* **1992**, *97*, 2571.
(22) Noodlemann, L.; Peng, C. Y.; Case, D. A.; Mouesca, J. M. *Coord. Chem. Rev.* **1995**, *144*, 199.
(23) Noodlemann, L.; Case, D. A. *Adv. Inorg. Chem.* **1992**, *38*, 423.
(24) Noodlemann, L.; Davidson, E. R. *Chem. Phys.* **1986**, *109*, 1.
(25) Noodlemann, L. *J. Chem. Phys.* **1981**, *74*, 5737.
(26) Cano, J.; Alemany, P.; Alvarez, S.; Verdaguer, M.; Ruiz, E. *Chem.*−*Eur. J.* **1998**, *4*, 476.
(27) Ruiz, E.; Cano, J.; Alvarez, S.; Alemany, P. *J. Am. Chem. Soc.* **1998**, *120*, 11122.
(28) Cano, J.; Ruiz, E.; Alemany, P.; Lloret, F.; Alvarez, S. *J. Chem. Soc., Dalton Trans.* **1999**, 1669.
(29) Ruiz, E.; Cano, J.; Alvarez, S.; Alemany, P. *J. Comput. Chem.* **1999**, *20*, 1391.
(30) Castro, I.; Calatayud, M. L.; Sletten, J.; Lloret, F.; Cano, J.; Julve, M.; Seitz, G.; Mann, K. *Inorg. Chem.* **1999**, *38*, 4680.
(31) Perdew, J. P.; Savin, A.; Burke, K. *Phys. Rev. A* **1995**, *51*, 4531.
(32) Miehlich, B.; Stoll, H.; Savin, A. *Mol. Phys.* **1997**, *91*, 527.
(33) Goursot, A.; Malrieu, J. P.; Salahub, D. R. *Theor. Chim. Acta* **1995**, *91*, 225.
(34) SAINT, version 5.0; Bruker Analytical X-ray Systems: Madison, WI, 1996.
(35) Sheldrick, G. M. *SADABS empirical absorption program*; University of Gottingen: Gottingen, Germany, 1996.
(36) Sheldrick, G. M. *SHELX-97*; University of Gottingen: Gottingen, Germany, 1997.

Table 1. Crystal Data and Structure Refinement for **1** and **3**

	1	3
empirical formula	$C_{26}H_{52}F_{12}N_8Ni_2O_2P_2$	$C_{38}H_{60}F_{12}N_8Ni_2O_2P_2 \cdot 2(CH_3)_2CO$
fw	916.12	1184.46
temp, K	173(2)	293(2)
wavelength, Å	0.710 73	0.710 73
space group	$P2_1/c$	$P2_1/c$
unit cell dimens, Å and deg	$a = 7.901(4)$	$a = 13.854(3)$
	$b = 13.597(6)$	$b = 17.469(4)$
	$c = 17.565(10)$	$c = 12.543(3)$
	$\alpha = 90$	$\alpha = 90$
	$\beta = 96.46(4)$	$\beta = 116.22(3)$
	$\gamma = 90$	$\gamma = 90$
V, Å^3	1875.0(17)	2723.2(9)
Z	2	2
d(calcd), Mg/m^3	1.623	1.444
abs coeff, mm^{-1}	1.187	0.838
reflcns collcd	4313	21 765
indpndnt reflcns	2577 [R(int) = 0.0810]	7994 [R(int) = 0.0719]
data/restraints/params	2577/12/242	7994/66/380
goodness-of-fit on F^2	0.963	0.852
final R indices [$I > 2\sigma(I)$]	R1 = 0.0564, wR2 = 0.0988	R1 = 0.0500, wR2 = 0.1039
R indices (all data)	R1 = 0.1230, wR2 = 0.1164	R1 = 0.1526, wR2 = 0.1320
largest diff peak and hole, e Å^{-3}	0.426 and −0.320	0.569 and −0.414

Scheme 1

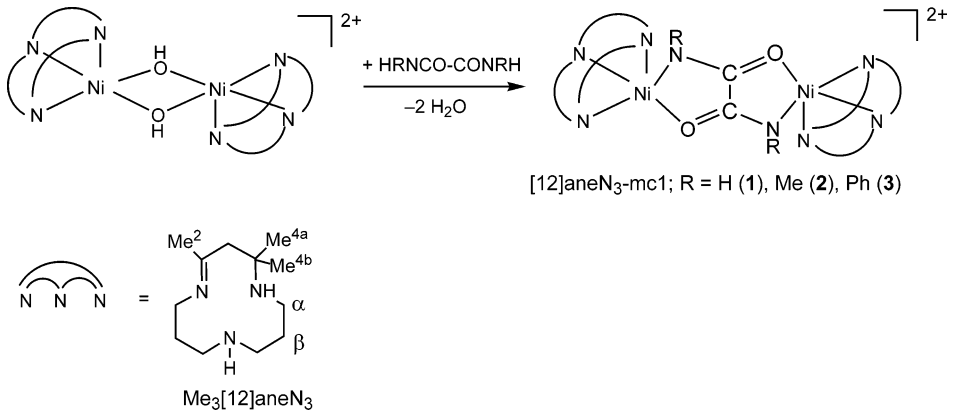

(substituent)oxamides (1:1 molar ratio) in acetone. The isolated complexes are sketched in Scheme 1.

The oxamides are deprotonated by the hydroxo groups of the dinuclear bis(μ-hydroxo) complexes and subsequently coordinate to the resulting $\{Ni(Me_3[12]aneN_3)\}^{2+}$ moiety affording the oxamidate-bridged dinuclear nickel(II) complexes with concomitant release of water. The basic $[Ni([12]aneN_3)(\mu\text{-}OH)]_2(PF_6)_2$ react with ligands containing acidic proton.[37] For this reason, $[Ni(Me_3[12]aneN_3)(\mu\text{-}OH)]_2(PF_6)_2$ reacts with oxamides producing H_2O and the complexes (**1**−**3**) containing the anion oxamidate as a nickel−nickel bound ligand. When the oxamides are deprotonated, both oxygen and nitrogen are coordinated to metal ions with a effective π-delocalization in the NCO fragments. These structural features have been confirmed by X-ray diffraction for complexes **1** and **3**.

Description of the Structures of 1 and 3. The crystal structure of the cation of complex $\{[Ni(Me_3[12]aneN_3)]_2(\mu\text{-}oa)\}(PF_6)_2$ (**1**) is shown in Figure 1, together with the atom numbering system. Bond distances and angles are given in Table 2. The complex lies on a crystallographic inversion center. The coordination about the nickel(II) ion can be regarded as a distorted square pyramid, the three nitrogen atoms of the N_3-macrocycle occupying the apical position (N3) and two adjacent equatorial ones (N1, N2), whereas the other two positions (O1, N4) correspond to the oxamidate group. The Ni atom is 0.266(3) Å out of the basal plane defined by N1, N2, N4, and O1 toward the axial nitrogen.

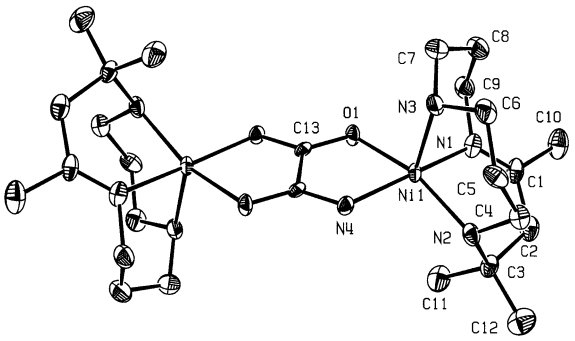

Figure 1. ORTEP plot of the cation of $\{[Ni(Me_3[12]aneN_3)]_2(\mu\text{-}oa)\}(PF_6)_2$ (**1**).

(37) (a) Santana, M. D.; García, G.; Rufete, A.; Sánchez, G.; Ramírez de Arellano, M. C.; López, G. *Inorg. Chem. Commun.* **1998**, *1*, 267. (b) Santana, M. D.; García, G.; Rufete, A.; Ramírez de Arellano, M. C.; López, G. *J. Chem. Soc., Dalton Trans.* **2000**, 267. (c) Santana, M. D.; García, G.; Pérez, J.; Molins, E.; López, G. *Inorg. Chem.* **2001**, *40*, 5701.

Table 2. Selected Bond Lengths (Å) and Angles (deg) for **1** and **3**

1		3	
Ni(1)−N(4)	2.014(5)	Ni(1)−N(4)	2.019(2)
Ni(1)−N(2)	2.042(7)	Ni(1)−N(3)	2.026(3)
Ni(1)−N(3)	2.056(6)	Ni(1)−N(1)	2.042(2)
Ni(1)−N(1)	2.074(6)	Ni(1)−N(2)	2.060(2)
Ni(1)−O(1)	2.052(5)	Ni(1)−O(1)	2.0435(19)
O(1)−C(13)	1.289(7)	O(1)−C(13)$^{\#2}$	1.262(3)
N(4)−C(13)$^{\#1}$	1.291(8)	N(4)−C(13)	1.313(3)
C(13)−C(13)$^{\#1}$	1.522(13)	C(13)−C(13)$^{\#2}$	1.518(5)
Ni(1)−Ni(1)$^{\#1}$	5.427(3)	Ni(1)−Ni(1)$^{\#2}$	5.384(4)
N(4)−Ni(1)−N(2)	95.0(2)	N(4)−Ni(1)−N(3)	110.64(10)
N(4)−Ni(1)−O(1)	80.7(2)	N(4)−Ni(1)−N(1)	95.73(9)
N(2)−Ni(1)−O(1)	160.5(2)	N(3)−Ni(1)−N(1)	94.74(10)
N(4)−Ni(1)−N(3)	99.4(2)	N(4)−Ni(1)−O(1)	81.58(8)
N(2)−Ni(1)−N(3)	100.6(2)	N(3)−Ni(1)−O(1)	89.94(9)
O(1)−Ni(1)−N(3)	98.9(2)	N(1)−Ni(1)−O(1)	175.20(9)
N(4)−Ni(1)−N(1)	167.5(2)	N(4)−Ni(1)−N(2)	146.18(10)
N(2)−Ni(1)−N(1)	89.9(3)	N(3)−Ni(1)−N(2)	100.99(10)
O(1)−Ni(1)−N(1)	90.9(2)	N(1)−Ni(1)−N(2)	93.22(10)
N(3)−Ni(1)−N(1)	91.0(2)	O(1)−Ni(1)−N(2)	86.93(9)

#1, $-x+1, -y+2, -z+1$. #2, $-x, -y+1, -z+2$.

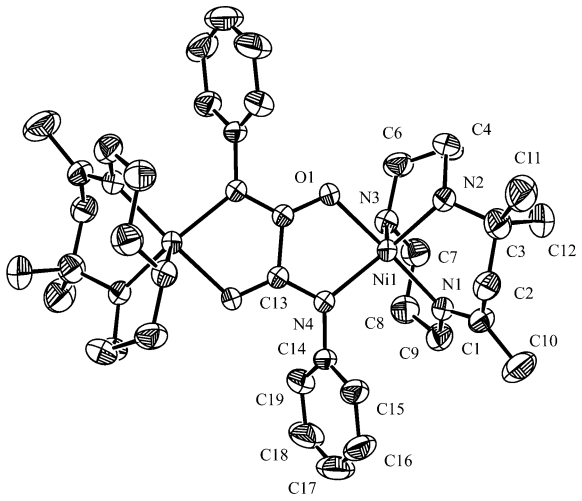

Figure 2. ORTEP plot of the cation of $\{[Ni(Me_3[12]aneN_3)]_2(\mu\text{-dpoa})\}(PF_6)_2 \cdot 2(CH_3)_2CO$ (**3**).

The rmsd of this plane is 0.078 Å. The basal plane forms a dihedral angle of 11.9(3)° with the plane of the bridge ligand. The Ni−Me_3[12]aneN_3 distances are not significantly different (Ni−N1, 2.074(6), Ni−N2, 2.042(7), Ni−N3, 2.056(6) Å) from those observed in pentacoordinate thionate complexes of nickel(II) containing an N_3-macrocycle.[37b] The $Ni-O_{oxamidate}$ bond distances are a little shorter than those observed in dinuclear octahedral Ni(II) complexes containing *trans*-oxamides[6] and in dinuclear complexes with square-planar and octahedral environment for Ni(II) containing *cis*-oxamidate.[8,9] However the $Ni-N_{oxamidate}$ bond distances are a little longer than those observed in the complexes mentioned above. The nickel−nickel separation, 5.427(3) Å, is longer than the distances reported for dinuclear Ni−Ni[6,8,9] and Ni−Cu[11] complexes with the bridging oxamidate ligand.

The structure of the cationic part of complex **3** is shown in Figure 2 with the atom numbering. Selected bond distances and angles are given in Table 2. The geometrical center of the oxamidate bridge is a crystallographic inversion center. The nickel atoms in **3** are coordinated in a distorted square pyramidal geometry to the nitrogen and oxygen atoms (N4, O1) of the deprotonated *N*,*N*′-diphenyloxamide and three nitrogen atoms (N1, N2, N3) of the Me_3[12]aneN_3 molecule. The Ni atom is 0.322(2) Å out of the basal plane (N1, N2, N4, and O1) toward the axial nitrogen, and the rmsd of this plane is 0.241 Å. The basal plane forms a dihedral angle of 13.6° with the plane of the bridging ligand. The nickel−nickel separation through the oxamidate bridge is 5.384 Å.

In pentacoordinate compounds, the geometry of the complex can be described by a structural index parameter τ [38] such that $\tau = (\beta - \alpha)/60°$, where β and α are the two largest angles ($\beta > \alpha$). Thus, the geometric parameter τ is applicable to pentacoordinate structures as an index of the degree of trigonality, within the structural continuum between trigonal bipyramidal (TBP) ($\beta - \alpha = 60°$, $\tau = 1$) and square pyramidal (SP) ($\beta - \alpha = 0°$, $\tau = 0$). Complex **1** has a τ value of 0.12 indicating a little distortion from perfect SP. However, complex **3** has a τ value of 0.48 and the environment around nickel atom is intermediate between square pyramidal and trigonal bipyramidal. Moreover, when the oxamides are deprotonated and both oxygen and nitrogen atoms are coordinated to metal ions, a more effective π-delocalization in the NCO fragment results, as evidenced in **1** by nearly identical N4−C13$^{\#1}$ and O1−C13 distances in the deprotonated coordinated amide, but in **3** the distances N4−C13 (1.313(3) Å) and O1−C13$^{\#2}$ (1.262(3) Å) are not nearly identical. These differences in geometry may be partly responsible for the apparent change in magnetic interaction. These structural features have already been observed in reported oxamide-containing copper(II)[39] or nickel(II)[6] complexes and are the reason for the remarkable efficiency of the oxamidate to transmit electronic effects when acting as a bridge.

Spectroscopic Study. The ^{1}H NMR spectra for complexes **1**−**3** show the resonance line pattern observed for the [12]-aneN_3-macrocycle ligand that has been assigned on the basis of previous studies of nickel macrocyclic complexes.[37] The α-methylene protons shift downfield whereas the β-methylene protons shift upfield with regard to the diamagnetic position probably because of spin polarization mechanisms.[40] Equatorial protons are expected to experience larger contact shifts than axial protons, and therefore, the most downfield resonances are due to α-CH_{eq} and the most upfield ones to β-CH_{eq}.[41] The isotropically shifted ^{1}H NMR signals observed for methyl groups (2-Me, 4-Me(a, b), and 9-Me-N) can be initially assigned by inspection of their peak areas as well as the methyl group of *N*,*N*′-dimethyloxamidate. The spectrum of the *N*,*N*′-diphenyloxamidate derivative **3** is similar to that of the corresponding oxamidate complex **1** in signals and magnitudes of contact shifts, but one striking difference is evident upon inspection of Figure 3 that some signals related to a given proton occur as doubled signals. The magnitude of contact shift differences for some α-CH protons and for 4-Me and 2-Me groups implies that these differences

(38) Rao, T. N.; Addison, A. W. *J. Chem. Soc., Dalton Trans.* **1984**, 1349.
(39) Lloret, F.; Julve, M.; Faus, J.; Journaux, J.; Philoche-Levisalles, M.; Jeannin, Y. *Inorg. Chem.* **1989**, *28*, 3702.
(40) Dei, A.; Wicholas, M. *Inorg. Chim. Acta* **1989**, *166*, 151.
(41) La Mar, G. N., Horrocks, W., Jr., Holm, R. H., Eds. *NMR of Paramagnetic Molecules*; Academic Press: New York, 1973; p 243.

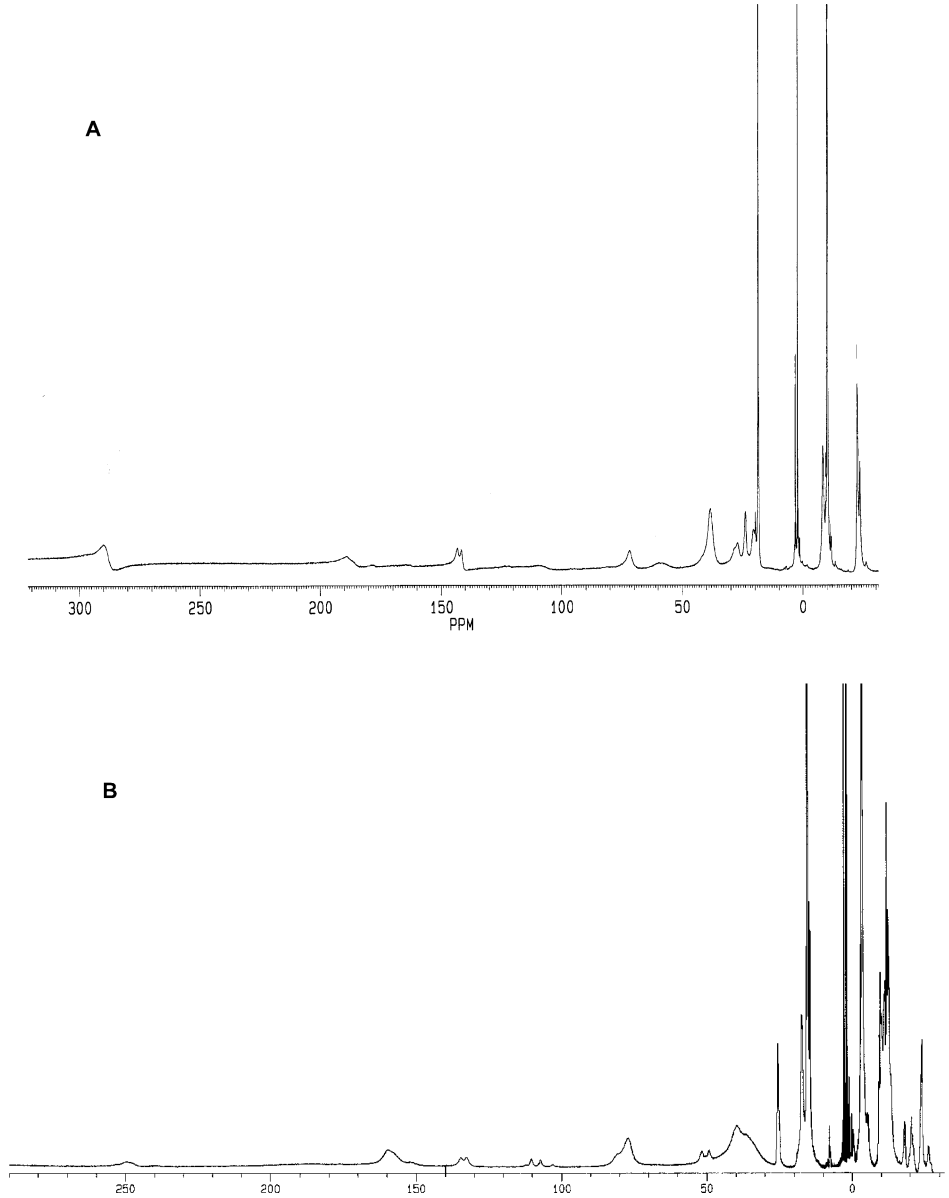

Figure 3. ^{1}H NMR spectra (in acetone-d_6 solution at room temperature) of **1** (A) and **3** (B).

arise from two distinct configurations. The intrinsically dissimilar forms are possibly further differentiated by a lack of free rotation of the phenyl groups about the C−N bond;[42] even so the presence of conformers in solution has been observed also by Curtis et al.[13a] and Dei et al.[40] in other complexes containing this Ni(II) [12]aneN_3-macrocycle moiety and has been attributed to the two possible reciprocal chiralities of nitrogen atoms. The NOESY spectrum of **3** (Figure 4) gave us valuable information to achieve the assignment of the phenyl protons of the *N*,*N*′-diphenyloxamidate. So the signal at 25.6 ppm connected through NOESY cross-peaks with signals at 17.5 (H_α), 15.4 (4-Me), and −3.1 ppm respectively should correspond to the *ortho* protons of the phenyl group, and the signals at −3.1 and −3.4 ppm could correspond to the *meta* and *para* protons, respectively. This specific assignment of these phenyl protons can be deduced from the inspection of the X-ray structure. This pattern could suggest that the *N*,*N*′-diphenyloxamidate display two spin delocalization mechanisms[43] through the OCN group (see below).

Magnetic Properties of 1−3. The temperature dependence of the $\chi_M T$ product [χ_M is the magnetic susceptibility/two Ni(II) ions] is shown in Figure 5. At room temperature, $\chi_M T$ is about 2.1 cm^3 mol^{-1} K for **1**−**3**, a value which is as expected for two $S = 1$ spin states. Upon cooling, this value decreases quickly and it vanishes at very low temperatures indicating the occurrence of a low-lying $S = 0$ state. The χ_M versus T plots of **1**−**3** (see inset of Figure 5) show rounded maxima at 76 (**1**), 58 (**2**), and 40 K (**3**). These features are characteristic of a relatively strong antiferromagnetic interaction between two single-ion triplet states.

(42) Holm, R. H.; Chakravorty, A.; Dudek, G. O. *J. Am. Chem. Soc.* **1963**, *85*, 821.

(43) Bertini, I.; Luchinat, C.; Parigi, G. *Solution NMR of Paramagnetic Molecules-Applications to Metallobiomolecules and Models*; Elsevier Science BV: Amsterdam, 2001; p 29.

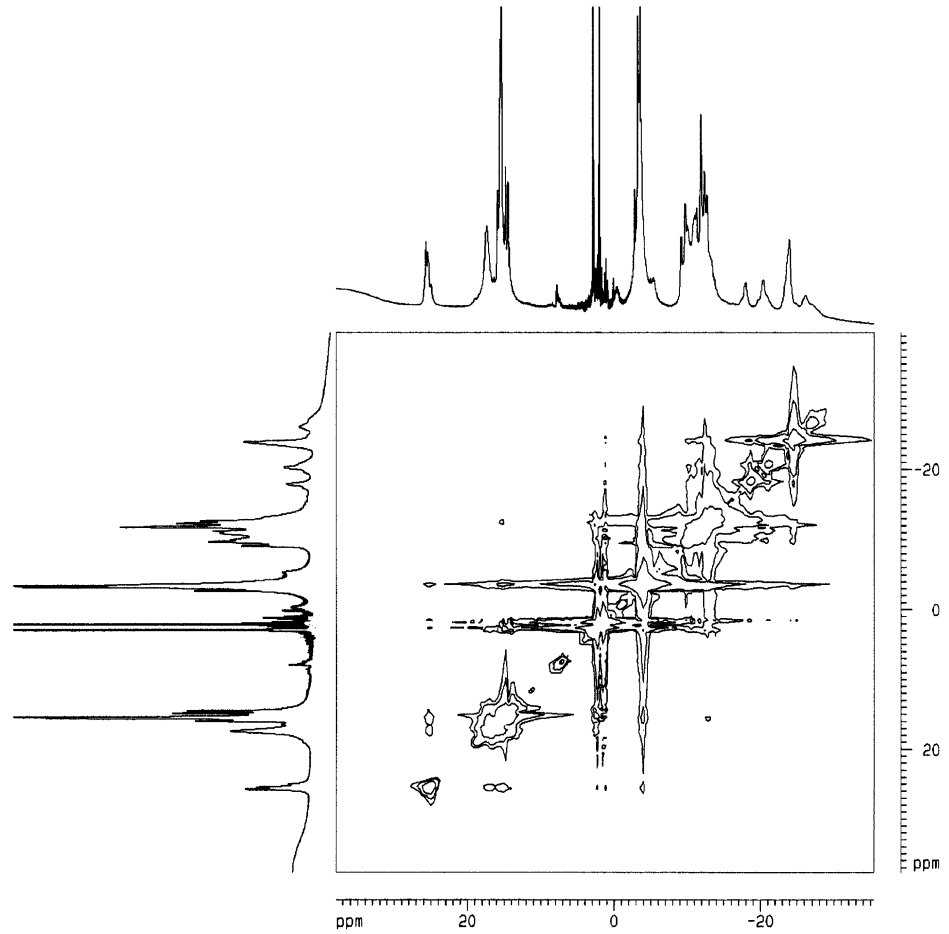

Figure 4. ^{1}H NOESY spectrum of **3** obtained at 400 MHz at 21 °C in acetone-d_6 solution. This map was collected with a 9 ms mixing time and 256 t_1 values (4096 scans each) using 1K data points in the F2 dimension; only the region relevant to assign resonances is shown in the top trace.

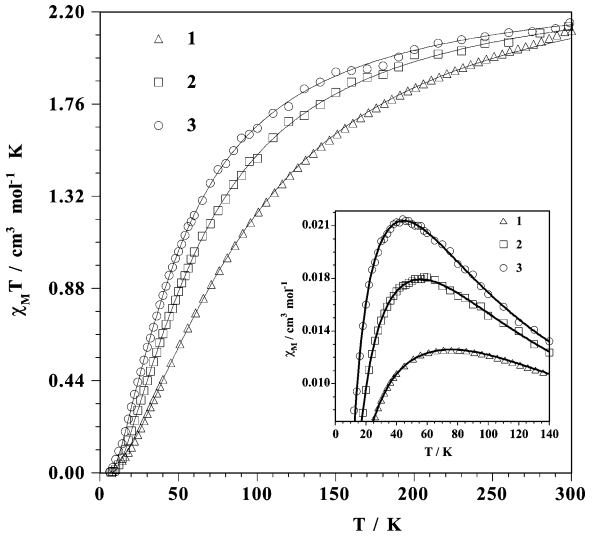

Figure 5. Thermal variation of the $\chi_M T$ product for **1**−**3**. [χ_M is the magnetic susceptibility/two Ni(II) ions.] The inset shows the susceptibility plots in the vicinity of the maximum. The solid lines are the bit fit curves through eq 1 (see text).

Consequently, we have analyzed the magnetic susceptibility of **1**−**3** by the expression for a nickel(II) dimer derived from the isotropic Hamiltonian of eq 1 ($S_A = S_B = 1$):

$$H = -JS_AS_B \qquad (1)$$

J is the intradimer magnetic interaction, and it is assumed that $g_x = g_y = g_z = g$. We have not considered the effect of the zero-field splitting on the magnetic behavior of **1**−**3** because it is expected to be negligible in the case of a large stabilization of the singlet ground state; that is, $-J \geq 20$ cm^{-1}.[44] Least-squares fit of the susceptibility data through eq 1 leads to $J = -57.0$ cm^{-1}, $g = 2.28$, and $R = 2.4 \times 10^{-5}$ for **1**, $J = -38.0$ cm^{-1}, $g = 2.20$, and $R = 2.1 \times 10^{-5}$ for **2**, and $J = -30.5$ cm^{-1}, $g = 2.18$, and $R = 2.3 \times 10^{-5}$ for **3**, respectively. R is the agreement factor defined as $R = \Sigma(\chi_{Mexptl}(i) - \chi_{Mcalcd}(i))^2/\Sigma(\chi_{Mexptl}(i))^2$. The calculated curves reproduce very well the magnetic data in the whole temperature range investigated.

As far as we are aware, this is the first report on the structure and magnetic properties of oxamidate-bridged dinuclear nickel(II) complexes where the nickel atom is five-coordinate. Usually, mononuclear oxamidate-containing nickel(II) complexes are diamagnetic square planar species due to the coordination of the strong-field amide nitrogen atoms.[3g,8,9,10b] Two strategies can be envisaged by the synthetic chemists to avoid this situation and prepare paramagnetic Ni(II) oxamidate complexes. The first one consists of moderating the strength of the ligand field of the oxamidate by fixing pendant groups on the amidate nitrogen atoms that

(44) (a) Duggan, M. D.; Barefield, E. K.; Hendrickson, D. N. *Inorg. Chem.* **1973**, *12*, 985. (b) De Munno, G.; Julve, M.; Lloret, F.; Derory, A. *J. Chem. Soc., Dalton Trans.* **1993**, 1179.

contain low-basicity donor atoms (case of *N*,*N*′-substituted oxamides) which can introduce some angular strain when bound to the nickel atom. The structure of the dinuclear nickel(II) compound $[Ni_2(glyox)(H_2O)_6]\cdot 4H_2O$ (H_4glyox = oxamide-*N*,*N*′-diacetic acid) where the oxamidate acts as a bridging bis-terdentate ligand illustrates this strategy.[6a] The nickel atom in this compound exhibits an slightly elongated octahedral environment with three atoms from glyox (one carboxylate oxygen, one amidate nitrogen, and one amidate oxygen) and a water molecule in the equatorial plane and two water molecules in the axial positions. A relatively strong antiferromagnetic interaction ($J = -25$ cm^{-1}) between the paramagnetic Ni(II) ions through the oxamidate bridge was found. The second one consists of blocking partially the coordination sphere of the nickel(II) ion by a polydentate ligand prior to its complexation with the oxamidate ligand. The macrocyclic ligand $Me_3[12]aneN_3$ allow us to illustrate this strategy. So, the highly stable $[Ni\{Me_3[12]aneN_3\}]^{2+}$ unit is found in the structurally characterized heterobimetallic complexes of formula $\{Ni(Me_3[12]aneN_3)Cu(apoa)\}(ClO_4)_2$[11] [$H_2$apoa = *N*,*N*′-bis(3-aminopropyl)oxamide] and $\{Ni(Me_3[12]aneN_3)Cu(pdmg)(EtOH)\}(ClO_4)_2$[45] [$H_2$pdmg = 3,9-dimethyl-4,8-diazaundeca-3,8-diene-2,10-dione dioxime]. The nickel atom in both compounds is paramagnetic and five coordinate with a stereochemistry intermediate between square pyramidal and trigonal bipyramidal: the three nitrogen atoms from the triaza macrocycle and either two oxamidate or two oximate oxygens form a distorted five-coordinate environment around the nickel atom. It seems that this macrocyclic ligand is specially suited to induce a unusual five-coordinate surrounding around the nickel(II) ion. The structures of the complexes **1** and **3** of this work (and most likely that of **2**) reinforce this observation.

The lack of magneto−structural studies on compounds similar to **1**−**3** precludes any comparison. However, the trend of the magnitude of the antiferromagnetic coupling in this family can be rationalized on simple magnetic orbital considerations on the basis of a DFT study. There are two important differences in this family of compounds: (i) a geometric distortion in the coordination sphere of metal ions; (ii) a different ligand substitution in the bridging ligand. The environment of each nickel(II) ion in the case of complex **1** is very close to a square pyramid, while the substitution of the hydrogen atom of the amidate nitrogen of **1** by a methyl (**2**) or a phenyl (**3**) group causes a significant modification of the stereochemistry of the nickel(II) ions from square pyramidal toward trigonal bipyramidal (τ values of 0.12 and 0.48 for **1** and **3**, respectively). Although these two effects are present together in these compounds, we can evaluate the influence of each one of them on the magnetic interaction by choosing the appropriate models. Thus, two models, with an oxamidate (model A) and a phenyl-substituted oxamidate (model B) as bridging ligands, have been built keeping in mind the respective experimental geometries (compounds **1** and **3**, respectively). For both models, the peripheral tridentate ligand is substituted by three ammonia groups and three

(45) Cervera, B.; Ruiz, R.; Lloret, F.; Julve, M.; Faus, J.; Muñoz, M. C.; Journaux, Y. *Inorg. Chim. Acta* **1999**, *288*, 57.

Chart 1

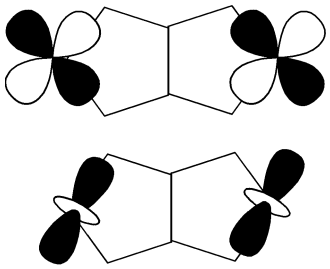

Table 3. Exchange Coupling Constants[a] Obtained from DFT Calculations for the Dinuclear Model Compounds of the Series A_i and B_i

i	A_i	B_i
1	−44.8	−36.9
2	−29.1	−23.0
3	−33.4	−31.1

[a] Values of J in cm^{-1}.

modifications of the environment of the metal ion are considered (they are noted A_i and B_i with $i = 1-3$). The environment for each nickel(II) ion in the model A_1 (Chart 1, top) is square pyramidal, the metal ion being placed in the plane of the bridging ligand, as in complex **1**. However, the metal coordination sphere corresponds to trigonal bipyramidal in the models A_2 and A_3 (also in B_2 and B_3): the *z* axis in A_2 (B_2) and A_3 (B_3) points toward either the oxamidate nitrogen (A_2 and B_2) or oxamidate oxygen (A_3 and B_3) atoms on both metal sites (Chart 1, bottom). Thus, compound **3** is nearer to model B_2 (and also A_2).

The calculation of the values of the exchange coupling constants for all six models is very interesting to understand the variation of J in **1**−**3**. The values of the exchange coupling constant found by DFT type calculations are shown in Table 3. A good agreement is observed between the calculated values and the experimental ones, supporting the validity of the models that we propose. A comparison between the J values in the A_i and B_i series reveals that the antiferromagnetic interactions are somewhat larger in the former ones. Thus, the attachment of organic groups at the oxamidate nitrogen modifies the energy and the distribution of the electronic density of the orbitals involved in the transmission of the magnetic exchange coupling through the oxamidate bridge. One can see that the replacement of the oxamidate hydrogen by the bulkier phenyl group causes a decrease of the antiferromagnetic interaction. As already seen in the oxalate-bridged dinuclear copper(II) complexes,[26] there is a strong dependency in the present series between the magnitude of the magnetic interaction and the relative arrangement of the magnetic orbitals respect to the bridging ligand. The understanding of this phenomenon here is more difficult because each nickel(II) ion has two magnetic orbitals [only one in the case of copper(II)]. To make easier this task, we only will consider the antiferromagnetic contributions that imply the shortest oxamidate NCO exchange pathway; the assumption, which is qualitatively reasonable given these contributions, is that these pathways must be the strongest ones. In the models A_1 and B_1, the strongest antiferromagnetic contribution involves a $d_{x^2-y^2}$ type magnetic orbital on

each metal center (see Chart 1, top). A weaker second contribution is present when the d_{z^2} type magnetic orbitals of the nickel(II) ions are considered.

In the case of the trigonal bipyramidal geometry shown by the A_2, A_3, B_2, and B_3 models (Chart 1, bottom), the main antiferromagnetic contribution is that, concerning the d_{z^2} type magnetic orbitals, the overlap between the parallel $d_{x^2-y^2}$ magnetic orbitals (which are perpendicular to the oxamidate plane) through the bridging oxamidato being very poor. If we focus thus on the orientation of the d_{z^2} magnetic orbital and keep in mind that most of its spin density lies on the *z* axis, the shortest oxamidate NCO exchange pathway connects one axial position (great spin density) from one metal ion with an equatorial one (poor spin density) at the other metal ion (Chart 1, bottom). This asymmetry with regard to what is observed for the $d_{x^2-y^2}$ orbital in A_1 and B_1 models decreases the antiferromagnetic contribution in the A_2, A_3, B_2, and B_3 cases as reflected by the corresponding calculated values of *J* (see Table 3). The somewhat different *J* values which are computed for A_2 and A_3 models (also in B_2 and B_3) are due to the different interaction of the metal orbitals with the oxygen and nitrogen donor atoms of the bridging oxamidate.

Finally, we have calculated the values of the exchange coupling constant for **1** and **3** using the experimental structures. The computed *J* values are -45.2 and -36.1 cm^{-1}, respectively. They are remarkably close to the experimental values [-57.0 (**1**) and -30.5 cm^{-1} (**3**)]. We have also calculated the *J* value for the structure of **3** but replacing the phenyl group in the oxamidate by a hydrogen atom. The computed *J* value is -41.3 cm^{-1}. The comparison of this result with those found for the complexes **1** and **3** allows us to substantiate the main factors that cause the decrease of the antiferromagnetic coupling when going from **1** to **3**. In summary, both the distortion of the coordination sphere of the metal ion and the inclusion of pendant organic groups on the bridging ligand play a relevant role on the magnetic interaction, the second factor being less important than the first one.

Acknowledgment. We thank the Fundación Séneca, CARM (project PI-32/00800/F.S./01), for financial support and the Ministerio Español de Ciencia y Tecnología for partial financial support through the research project BQ2001-2928.

Supporting Information Available: X-ray crystallographic files for compounds **1** and **3** in CIF format. This material is available free of charge via the Internet at htpp://pubs.acs.org.

IC030050F